performed up to $|h|=38$ with Bertaut's method (6), in order to obtain the same relative precision; and this requires 8 h 45 min of calculation time. All the calculations were made on a 16-bit minicomputer (DEC PDP11/45).

In the biochlorites, the smallest interatomic distance d is the O–H distance of about 1 Å; thus, the radius R of Bertaut's method (6) must be about 0·5 Å. Because all other O–cation distances are greater than 1 Å, a more rapid convergence is obtained with the 'multi-radii method' (of § 2.4.1), as shown in Fig. 2 for the case of biotite. With the 'overlapping method' (§ 2.4.2) we may choose $R>0{\cdot}5$ Å; the convergence is similar to that of the 'multi-radii method' if $R=0{\cdot}75$ Å, and it is more rapid if $R>0{\cdot}75$ Å (Fig. 2*a*). This is also illustrated in Fig. 3, in the case of 1-1 biochlorite: with $R=4$ Å, the series E_1 converges very rapidly and the finite sum E_3 requires only 15 min of calculation time. Higher values of R give a better convergence for E_1, but a longer calculation time for E_3.

References

BERTAUT, F. (1952). *J. Phys. Radium*, **13**, 499-505.
BORN, M. & LANDÉ, A. (1918). *Verh. Dtsch. Phys. Ges.* **20**, 210-216.
EWALD, P. P. (1921). *Ann. Phys. (Leipzig)*, **64**, 253-287.
GIESE, R. F. (1975). *Z. Kristallogr.* **141**, 138-144.
IIJIMA, S. & ZHU, J. (1982). *Am. Mineral.* **67**, 1195-1205.
JENKINS, H. D. B. & HARTMAN, P. (1979). *Philos. Trans. R. Soc. London Ser. A*, **293**, 169-208.
JOSWIG, W., FUESS, H., ROTHBAUER, R., TAKEUCHI, Y. & MASON, A. (1980). *Am. Mineral.* **65**, 349-352.
KNIPE, R. J. (1981). *Tectonophysics*, **78**, 249-272.
MADELUNG, E. (1918). *Phys. Z.* **19**, 524-532.
MARESCH, W. V., MASSONNE, H.-J. & CZANK, M. (1985). *Neues Jahrb. Mineral. Abh.* **152**, 79-100.
OLIVES, J. (1985*a*). *Terra Cognita*, **5**, 226.
OLIVES, J. (1985*b*). *Bull. Minéral.* **108**, 635-641.
OLIVES, J. (1985*c*). *J. Phys. (Paris) Lett.* **46**, 1143-1149.
OLIVES, J. & AMOURIC, M. (1984). *Am. Mineral.* **69**, 869-871.
OLIVES, J., AMOURIC, M., DE FOUQUET, C. & BARONNET, A. (1983). *Am. Mineral.* **68**, 754-758.
PAGE, R. H. & WENK, H. R. (1979). *Geology*, **7**, 393-397.
RAYNER, J. H. (1974). *Mineral. Mag.* **39**, 850-856.
VEBLEN, D. R. (1983). *Am. Mineral.* **68**, 566-580.
VEBLEN, D. R. & FERRY, J. M. (1983). *Am. Mineral.* **68**, 1160-1168.

Acta Cryst. (1986). A**42**, 344-348

Comparison of an *Umweganregung* Pattern, Measured on an Automatic Single-Crystal Diffractometer, With Calculated Patterns

BY ELISABETH ROSSMANITH

Mineralogisch-Petrographisches Institut der Universität Hamburg, Grindelallee 48, *D*-2000 *Hamburg* 13, *Federal Republic of Germany*

(*Received* 20 *August* 1985; *accepted* 24 *March* 1985)

Abstract

The ψ scan of the forbidden 003 reflection of Zn, measured with an automatic single-crystal diffractometer, using Cu $K\alpha$ radiation, is compared with the calculated and plotted *Umweganregung* pattern for Cu $K\alpha_1$ and Cu $K\alpha_2$ radiation. The intensities of the *Umweganregung* peaks are calculated on the basis of the kinematical theory. When the Lorentz factors for both scans involved in the measurement (the θ scan and the ψ scan) are taken into account, excellent agreement between measured and calculated intensities is obtained. The width of the *Umweganregung* peaks can be explained by replacing the reciprocal-lattice points by spheres in reciprocal space.

Introduction

In the last few years interest in weak high-order reflections measured with X-rays of short wavelength has increased in structure analysis. Multiple diffraction systematically increases the weak intensities and falsifies the intensity data sets. The influence of the simultaneous reflections on weak intensities must therefore be investigated thoroughly, using the experimental arrangement of the automatic single-crystal diffractometer employed in structure analysis.

Since Renninger (1937) carried out a systematic investigation into the multiple diffraction phenomenon in the ψ-scanning pattern of the 222 reflection of diamond, many papers on this topic have been published. An extensive bibliography of this subject is given by Post (1975, 1976) and in papers cited therein. Recently the computer program *UMWEG* was published by the author (Rossmanith, 1985); this program is based mainly on the geometrical considerations of Cole, Chambers & Dunn (1962).

Simultaneous diffraction occurs when three or more reciprocal-lattice points lie simultaneously on

0108-7673/86/050344-05$01.50

the Ewald sphere. If (apart from the origin of the reciprocal lattice) two further reciprocal-lattice points lie on the Ewald sphere, the intensity of the primary reflection hkl is influenced by the second reflection $h_1k_1l_1$, which is called the operative reflection. There is always a third reflection $h-h_1, k-k_1, l-l_1$, called the cooperative reflection, which reflects part of the intensity of the operative reflection back in the direction of the primary reflection. Whether the intensity of the primary reflection is increased or attenuated depends on the reflectivities of the three cooperating reflections.

If the Lorentz and polarization factors are neglected and small or moderate absorption is assumed, the change in the integrated intensity ΔI_{prim} of the primary reflection, caused by the presence of secondary beams, is given by Post [1976; formula (1)] as

$$\Delta I_{\text{prim}} \propto \sum_{\text{op}} (-Q_{\text{prim}}Q_{\text{op}} - Q_{\text{prim}}Q_{\text{coop}} + Q_{\text{op}}Q_{\text{coop}}). \quad (1)$$

Q_{prim}, Q_{op} and Q_{coop} are the effective reflectivities of the primary, the operative and the cooperative reflections respectively. The summation in (1) extends over all secondary beams.

Prager (1971) stated on p. 565 of his paper: 'Accordingly, when several secondary reflections are simultaneously excited, each one can be treated independently as regards its effect on R_D. [$R_D = \Delta I_{\text{prim}}/I_{\text{prim}}$.] Therefore, if this result may be assumed to hold for spherical crystals, it is sufficient hereafter to treat only double diffraction, on the understanding that approximate results for higher-order diffraction may be obtained by summing over secondary reflections.'

In the case of a forbidden primary reflection, (1) therefore reduces to

$$\Delta I_{\text{prim}} \propto Q_{\text{op}}Q_{\text{coop}} \propto F_{\text{op}}^2 F_{\text{coop}}^2. \quad (2)$$

F_{op} and F_{coop} are the structure factors multiplied by the temperature factors for the operative and cooperative reflections respectively.

Experimental

The *Umweganregung* pattern of the forbidden 003 reflection (Fig. 1) of the h.c.p. Zn single crystal (space group $P6_3/mmc$) was measured with the automatic single-crystal diffractometer CAD4 by Enraf–Nonius using the ψ-scan technique under the usual conditions of intensity measurements in structure analysis.

A Zn sphere with diameter 92 μm was used as sample. The 002 reflection of a graphite single crystal was used for monochromatization of the primary X-ray beam. A 1·1 mm pinhole at the ends of the collimator between the small single-crystal sphere and the monochromator limited the divergence of the incident beam impinging on the crystal to 32′. The distances between the crystal and the ends of the collimator were 119·5 and 47 mm.

For each azimuthal angle ψ the diffractometer setting angles φ, χ and ω were calculated using formulae given, for example, by Busing & Levy (1967). For ten steps per degree in ψ the intensity was measured in a θ–2θ scan with 10 min measuring time per ψ step. The integrated intensity over the θ–2θ scan is plotted against ψ in Fig. 1. Because of the symmetry the asymmetric region of the pattern extends for 30°.

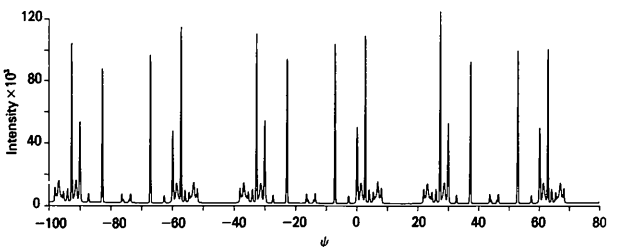

Fig. 1. Measured ψ scan of the forbidden 003 reflection of Zn. ψ step: 0·1°.

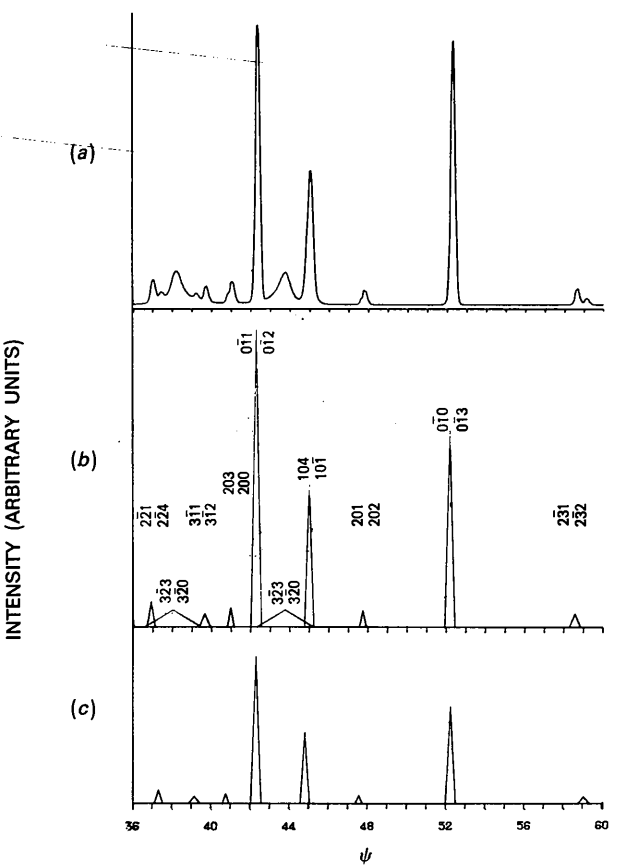

Fig. 2. Measured and calculated ψ scans of the forbidden 003 reflection of Zn. (*a*) Measured ψ scan, step width 0·02°. (*b*) Calculated ψ scan for Cu $K\alpha_1$. (*c*) Calculated ψ scan for Cu $K\alpha_2$.

A region of 25° in ψ was measured once more with 0·02° steps in ψ and 10 min measuring time per ψ step. The result is given in Fig. 2(*a*).

Calculations

(*a*) *Geometrical condition for simultaneous diffraction*

The program *UMWEG* (Rossmanith, 1985) calculates the condition for the appearance of *Umweganregung* peaks following the method given by Cole, Chambers & Dunn (1962). The angle ψ between a reference direction perpendicular to the scattering vector of the primary reflection and the projections on planes normal to the scattering vector of the primary reflection for the scattering vectors of all the possible operative reflections is estimated, giving the positions of the triangles representing the peaks in the *Umweganregung* patterns [Figs. 2(*b*) and (*c*)]. In the case of the 003 reflection of Zn, [100] was selected as the reference direction. The operative and cooperative reflections are checked against the conditions limiting possible reflections and are rejected, if systematically absent.

(*b*) *Intensity*

The formula used by the program *UMWEG* for calculation of the intensity change ΔI_{prim} is that given in (2), derived in the framework of the kinematical theory, taking into consideration the polarization and Lorentz factors and is valid only for primary reflections forbidden by space group or special position as well as for very weak reflections, assuming that the structure factor of the primary reflection is equal or nearly equal to zero.

$$\Delta I_{\text{prim}} \propto (F_{\text{op}} F_{\text{coop}})^2 (p_{\text{op,coop}}/p_{\text{prim}}) \times (L_{\text{op}}^2 + L_{\text{coop}}^2)^{-1/2} L_\beta^{-1}, \quad (3)$$

where

$$p_{\text{op,coop}} = \tfrac{1}{2}[\cos^2 2\theta_{\text{op}} + \cos^2 2\theta_{\text{coop}} + (\cos 2\theta_{\text{prim}} - \cos 2\theta_{\text{op}} \cos 2\theta_{\text{coop}})^2], \quad (3a)$$

$$p_{\text{prim}} = \tfrac{1}{2}(1 + \cos^2 2\theta_{\text{prim}}), \quad (3b)$$

$$L_{\text{op}} = 1/\sin 2\theta_{\text{op}}, \qquad L_{\text{coop}} = 1/\sin 2\theta_{\text{coop}}, \quad (3c)$$

$$L_\beta = \sin\beta(\cos\theta_{\text{prim}}) H_n. \quad (3d)$$

The angles θ_{op}, θ_{coop} and θ_{prim} are the Bragg angles for the operative, cooperative and primary reflections. H_n and β are defined in Fig. 3, which will be explained in the next section. Whereas the formulae given by Zachariasen (1965), Prager (1971) and Post (1976) for $p_{\text{op,coop}}$ are all identical to (3*a*), the formulae given by these authors for p_{prim}, L_{op} and L_{coop} differ from one another.

The intensity change was therefore calculated for the different Lorentz and polarization factors given by these three authors. L_β was set equal to 1, as done by these authors, and it was found that only the intensity formula using the L_{op} and L_{coop} given by Post (1976) and the p_{prim} given by Prager (1971) resulted in tolerable agreement between observed and calculated intensities. The respective formulae are given in (3).

The disagreement between measured and observed intensities was found to depend on the angle β. It was therefore concluded that two Lorentz factors have to be taken into consideration. The first is due to the θ–2θ scan (L_{op}, L_{coop}) and the second Lorentz factor is due to the ψ scan (L_β) and is given by Post (1975).

The heights of the triangles in Figs. 2(*b*) and (*c*) are proportional to the calculated intensities. The calculated intensities are also given in Tables 1 and 2. As can be seen from the tables, all the *Umweganregung* peaks of Fig. 2 are due to four-beam interaction. If the intensities of the *Umweganregung* peaks are calculated with (1), the intensity contributions from the two operative reflections have to be summed. The summation reduces to the multiplication of one intensity contribution by a factor 2, because the intensity contributions of the two operative reflections are calculated to be identical (Tables 1 and 2). In the special case of the 003 reflection of Zn, therefore, the *Umweganregung* pattern can be calculated by (3) instead of (1).

(*c*) *Peak width*

The peak width of the reflection at $\psi = 38{\cdot}02°$ is very much broader than the other reflections in Fig. 2(*a*). The enlargement of the peak width and the intensity, which is much higher than calculated, can be explained from Fig. 3, which is based on Fig. 4 of Post (1975).

R_0 is the radius of the Ewald sphere; H_n is that component of the reciprocal-lattice vector belonging to the operative reflection which is normal to the reciprocal-lattice vector belonging to the primary reflection; r is the radius of the circle formed by the intersection of the Ewald sphere with the plane normal to the reciprocal-lattice vector belonging to the primary reflection, and which passes through the reciprocal-lattice point belonging to the operative reflection. Each lattice point passes the Ewald sphere twice during a ψ scan, and the difference between the corresponding ω values is equal to 2β.

In Fig. 3 the reciprocal-lattice points are replaced by spheres with radius ε in the reciprocal space. $\delta\beta$ is the angle between the two points, when the sphere with radius ε touches the Ewald sphere the first and the last time during a ψ scan. The angle $\delta\beta$ can be calculated from

$$\delta\beta = 2(\arccos\{[(R_0 \cos\theta_{\text{prim}})^2 + H_n^2 - (r+\varepsilon)^2] \times (2R_0 \cos\theta_{\text{prim}} H_n)^{-1}\} - \beta). \quad (4)$$

The calculated values for $\delta\beta$ are given in Tables 1

Table 1. *Calculated ψ scan; results for* Cu $K\alpha_1$ *radiation* (1·5406 Å)

Operative reflection					Cooperative reflection								
h	k	l	F	θ	h	k	l	F	θ	ΔI_{prim}	$\delta\beta$	β	ψ
2	−2	−1	23·52	43·26	−2	2	4	7·65	65·98	8·62	0·42	23·09	36·91
2	−2	4	7·65	65·98	−2	2	−1	23·52	43·26	8·62	0·42	23·09	36·91
3	−2	3	12·46	87·46	−3	2	0	9·83	61·98	5·58	2·87	2·87	38·02
3	−2	0	9·83	61·98	−3	2	3	12·46	87·46	5·58	2·87	2·87	38·02
3	−1	1	16·43	63·69	−3	1	2	8·53	69·42	4·36	0·57	20·54	39·65
3	−1	2	8·53	69·42	−3	1	1	16·42	63·69	4·36	0·57	20·54	39·65
2	0	3	17·13	54·58	−2	0	0	14·16	41·86	6·31	0·36	40·98	40·98
2	0	0	14·16	41·86	−2	0	3	17·13	54·58	6·31	0·36	40·98	40·98
0	−1	1	37·52	21·61	0	1	2	18·61	27·17	100·00	0·54	77·72	42·28
0	−1	2	18·61	27·17	0	1	1	37·52	21·61	100·00	0·54	77·72	42·28
3	−2	3	12·46	87·46	−3	2	0	9·83	61·98	5·58	2·87	2·87	43·76
3	−2	0	9·83	61·98	−3	2	3	12·46	87·46	5·58	2·87	2·87	43·76
1	0	4	10·88	45·02	−1	0	−1	37·52	21·61	48·60	0·47	44·99	44·99
1	0	−1	37·52	21·61	−1	0	4	10·88	45·02	48·60	0·47	44·99	44·99
2	0	1	23·52	43·26	−2	0	2	12·02	47·44	5·45	0·35	47·74	47·74
2	0	2	12·02	47·44	−2	0	1	23·52	43·26	5·45	0·35	47·74	47·74
0	−1	0	22·84	19·49	0	1	3	25·48	35·07	66·48	0·51	67·82	52·18
0	−1	3	25·48	35·07	0	1	0	22·84	19·49	66·48	0·51	67·82	52·18
2	−3	1	16·43	63·69	−2	3	2	8·53	69·42	4·36	0·57	20·54	58·57
2	−3	2	8·53	69·42	−2	3	1	16·43	63·69	4·36	0·57	20·54	58·57

Table 2. *Calculated ψ scan; results for* Cu $K\alpha_2$ *radiation* (1·5444 Å)

Operative reflection					Cooperative reflection								
h	k	l	F	θ	h	k	l	F	θ	ΔI_{prim}	$\delta\beta$	β	ψ
2	−2	−1	23·52	43·39	−2	2	4	7·65	66·30	8·79	0·43	22·67	37·33
2	−2	4	7·65	66·30	−2	2	−1	23·52	43·39	8·79	0·43	22·67	37·33
3	−1	1	16·43	63·98	−3	1	2	8·53	69·80	4·51	0·58	20·05	39·16
3	−1	2	8·53	69·80	−3	1	1	16·42	63·98	4·51	0·58	20·05	39·16
2	0	3	17·13	54·78	−2	0	0	14·16	41·99	6·35	0·36	40·77	40·77
2	0	0	14·16	41·99	−2	0	3	17·13	54·78	6·35	0·36	40·77	40·77
0	−1	1	37·52	21·67	0	1	2	18·61	27·25	100·00	0·54	77·69	42·31
0	−1	2	18·61	27·25	0	1	1	37·52	21·67	100·00	0·54	77·69	42·31
1	0	−1	37·52	21·67	−1	0	4	10·88	45·16	48·94	0·47	44·81	44·81
1	0	4	10·88	45·16	−1	0	−1	37·52	21·67	48·94	0·47	44·81	44·81
2	0	1	23·52	43·39	−2	0	2	12·02	47·59	5·44	0·36	47·57	47·57
2	0	2	12·02	47·59	−2	0	1	23·52	43·39	5·44	0·36	47·57	47·57
0	−1	0	22·84	19·54	0	1	3	25·48	35·17	66·54	0·51	67·75	52·25
0	−1	3	25·48	35·17	0	1	0	22·84	19·54	66·54	0·51	67·75	52·25
2	−3	1	16·43	63·98	−2	3	2	8·53	69·80	4·51	0·58	20·05	59·06
2	−3	2	8·53	69·80	−2	3	1	16·43	63·98	4·51	0·58	20·05	59·06

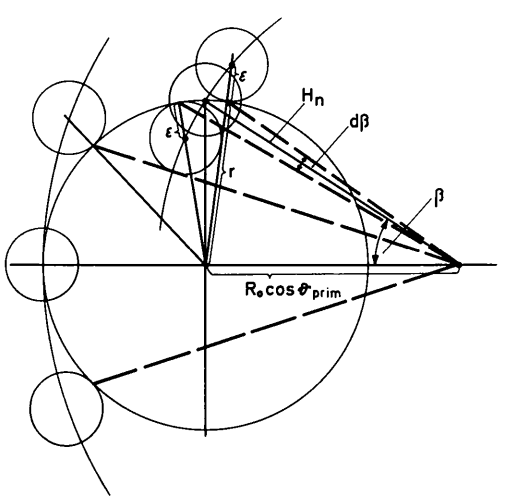

Fig. 3. Explanation of peak broadening, arising from the replacement of the reciprocal-lattice points by spheres.

and 2 and were used as the basis of the peak triangles in Figs 2(*b*) and (*c*). $\varepsilon = 0{\cdot}0018$ Å^{-1} was estimated by trial and error to fit the measured peak width. The measured peak width is influenced by the mosaic spread of the crystal, the divergence of the incident beam and the superposition of the peaks belonging to Cu $K\alpha_1$ and Cu $K\alpha_2$. Nevertheless, the peak widths calculated in the approximation (4) compare well with the measured peak width given in Fig. 2(*a*). In particular, the broadening of the peaks at $\psi = 38{\cdot}02$ and 43·76°, which can be identified as belonging to the $3\bar{2}3$ and $3\bar{2}0$ reflections with $\beta = 2{\cdot}87°$ (see Table 1) can now be understood. The peak starts at $\psi \simeq 36{\cdot}5°$, rising to peaks at $\psi = 36{\cdot}9$ and 37·33°, reaches its first maximum, declines and rises once more to reach the second maximum at $\psi \simeq 43{\cdot}76°$. The fact that the intensity does not reach the background value for ψ between 40 and 42° can be explained by the contribution to the intensity from the Cu $K\alpha_2$

radiation. The reciprocal-lattice points $3\bar{2}3$ and $3\bar{2}0$ do not pass the Ewald sphere belonging to the wavelength of Cu $K\alpha_2$, but when the reciprocal-lattice points are replaced by spheres, these spheres touch the Ewald sphere of Cu $K\alpha_2$ and contribute to the intensity in the above-mentioned region.

Comparison of measured and calculated *Umweganregung* patterns

Fig. 2(*b*) is calculated for Cu $K\alpha_1$ radiation, Fig. 2(*c*) for Cu $K\alpha_2$ radiation. ψ is zero in the [100] direction. With these two diagrams it is possible to index all *Umweganregung* peaks of the measured pattern in Fig. 2(*a*). The indices of the operative and cooperative reflections are given in Tables 1 and 2 together with their Bragg angles and structure factors. The zero point for ψ in the measured diagram is chosen arbitrarily.

The leftmost peak in Fig. 2(*a*) is built up of the two operative reflections $2\bar{2}\bar{1}$ and $2\bar{2}4$ with Cu $K\alpha_1$ radiation. The second peak belongs to the same reflections, but for Cu $K\alpha_2$ radiation. The difference in ψ for these two peaks is $\psi_{\alpha_1} - \psi_{\alpha_2} = -0{\cdot}42°$, as can be calculated from values in Tables 1 and 2. The third peak is the peak discussed above, having a respective triangle in Fig. 2(*b*) only.

Despite the difficulty of correcting for the superposition of the Cu $K\alpha_1$ and Cu $K\alpha_2$ peaks and disregarding the problematical second peak in Table 1, one finds that the comparison of the measured and calculated intensities gives surprisingly good agreement. The disagreement between the measured and calculated intensities for the peak at $\psi = 52{\cdot}18°$ is probably due to experimental shortcomings. As can be seen in Fig. 1 the intensity ratio of the two highest peaks varies between 1 : 0·7, in good agreement with the theory, in the range 20–40° and 1 : 1 in the ψ range 50–70°, owing to inadequate measurements.

Recently Soejima, Okazaki & Matsumoto (1985) referred to a similar program for the simulation of ψ scanning.

The author is grateful to Dr G. Adiwidjaja for performing the measurements.

References

BUSING, W. R. & LEVY, H. A. (1967). *Acta Cryst.* **22**, 457–464.
COLE, H., CHAMBERS, F. W. & DUNN, H. M. (1962). *Acta Cryst.* **15**, 138–144.
POST, B. (1975). *J. Appl. Cryst.* **8**, 452–456.
POST, B. (1976). *Acta Cryst.* A**32**, 292–296.
PRAGER, P. R. (1971). *Acta Cryst.* A**27**, 563–569.
RENNINGER, M. (1937). *Z. Phys.* **106**, 141–176.
ROSSMANITH, E. (1985). *Z. Kristallogr.* **171**, 253–254.
SOEJIMA, Y., OKAZAKI, A. & MATSUMOTO, T. (1985). *Acta Cryst.* A**41**, 128–133.
ZACHARIASEN, W. H. (1965). *Acta Cryst.* **18**, 705–710.

Acta Cryst. (1986). A**42**, 348–352

Experimental Observation of the Borrmann Pyramid – the Borrmann Fan for Four-Beam Transmission of X-rays*

BY CÍCERO CAMPOS

Instituto de Física, Universidade Estadual de Campinas, Campinas, SP 13100, *Brazil*

AND SHIH-LIN CHANG†

Instituto de Física, Universidade Estadual de Campinas, Campinas, SP 13100, *Brazil, and Department of Physics, National Tsing Hua University, Hsinchu, Taiwan* 300

(*Received* 16 *October* 1985; *accepted* 1 *April* 1986)

Abstract

The polyhedron which confines the Poynting vectors of *N*-beam transmissions in crystal space is referred to as the Borrmann pyramid. The observation of this Borrmann pyramid is realized from the diffraction images of the four-beam, (000)(220)($2\bar{2}0$)(400), transmission case of silicon single crystals for Mo $K\alpha$. The directions of the Poynting vectors for the eight modes of wave propagation involved and the diffraction images are calculated. These calculations confirm the experimental observations. The variation of the direction of the Poynting vector for each mode is also reported.

* This work forms part of the PhD dissertation of CC.

† Present address: National Tsing Hua University.

0108-7673/86/050348-05$01.50